

Evidence of B- and Si-type magnetic relaxations in Co-based amorphous alloys

P. Vojtanik,* R. Andrejco, and R. Varga

Institute of Physics, Faculty of Sciences, P.J. Safarik University, Park Angelinum 9, 041 54 Kosice, Slovakia

(Received 30 October 2003; published 31 August 2004)

The kinetics of the structural magnetic relaxations (MRs) in the Co-based amorphous alloys has been investigated by magnetic after-effect spectroscopy. The experimental evidence and characterization of two types of MRs in the amorphous $\text{Co}_{75}\text{B}_{25}$ and $\text{Co}_{75}\text{Si}_{15}\text{B}_{10}$ alloys are rendered in this work. The binary CoB alloy shows only the B-type MR with the most probable energy of the activation energy spectrum $Q^* = 1.35$ eV and the preexponential factor $\tau_0 = 2 \times 10^{-17}$ s. In the ternary CoSiB amorphous alloy, the additional Si-type MR with $Q^* = 1.96$ eV and $\tau_0 = 6 \times 10^{-18}$ s occurs. Low-temperature annealing shifts either of the relaxation parameters of both alloys to higher values. Roles of the free volumes, the dimension, and affinity of the B and Si atoms for Co in the MR are discussed.

DOI: 10.1103/PhysRevB.70.052407

PACS number(s): 75.50.Kj, 75.60.Lr, 81.40.Ef

The structural magnetic relaxation significantly influences the magnetic properties, processibility, and stability of the amorphous alloys. The Co-based amorphous alloys play an important role in technical applications because of their excellent soft magnetic properties.^{1,2} They exhibit good processibility by the magnetic annealing,³ which the atomic mechanism lies in the magnetic relaxation (MR). A powerful tool for investigating the MR is magnetic after-effect (MAE) spectroscopy.⁴

There are two theoretical approaches to MAE in the amorphous alloys. The micromagnetic model of the MR⁵ is based on the reorientations of the atom-pair axes near free volumes to the directions related to the local magnetizations (Fig. 1). A driving force for the reorientation is a reduction of the interaction energy ε of a given atom pair with the local magnetization

$$\Delta\varepsilon = \varepsilon_0(\cos^2 \varphi_2 - \cos^2 \varphi_1) < 0, \quad (1)$$

where φ_1 and φ_2 denote the initial and final angles between the atom-pair axis and the local magnetization, ε_0 is the local interaction energy consisting from exchange (ε^{ex}), spin-orbit (ε^K), and magnetoelastic (ε^{ex}) parts, $\varepsilon_0 = \varepsilon^{ex} + \varepsilon^K + \varepsilon^{el}$. Each atom pair acts as an individual two-level system. Assuming the first-order reaction, the time-temperature dependence of the reluctivity influenced by the MR can be expressed by the equation⁶

$$r(t, T) = r_0(T) + \Delta r \cdot \int_0^\infty p(\tau)(1 - e^{-t/\tau})d\tau, \quad (2a)$$

$$\tau = \tau_0 \exp(Q/kT), \quad (2b)$$

$$\tau_0 = \tau_{00} \exp(-S/k), \quad (2c)$$

where $r_0(T)$ is reluctivity at $t=0$, $\Delta r \sim n_0$ is the maximum reluctivity change (n_0 —concentration of mobile atom pairs), $p(\tau)$ is the distribution function of relaxation times τ , τ_0 is the preexponential factor, Q is the activation energy, k is the Boltzmann's constant, τ_{00} is a constant of the order of 10^{-13} s related to Debye frequency, and S is the activation entropy.

By the magnetostrictive model,⁷ the magnetostriction of alloy contributes to the MAE level and the MAE appears as independent of the actual alloy composition. The possible role played by the compositions of the amorphous and nanocrystalline alloys in the MRs is not definitely clarified.^{8,9} It looks to be reasonable to start an investigation of the MR in Co-based amorphous alloys with a binary CoB alloy.¹⁰ The only composition of the CoB-based amorphous alloy in which the atom-scale mechanism of the MAE was suggested is the hydrogen-charged $\text{Co}_{75}\text{Si}_{15}\text{B}_{10}$.¹¹ At 190 K, a hydrogen-related relaxation process with a mean activation energy of 0.42 eV was observed. The amorphous CoZr alloy shows an MAE peak from the atom-pair reorientations at 325 K.¹²

In this report we are dealing with the MRs in simple representative Co-based amorphous alloys— $\text{Co}_{75}\text{B}_{25}$ and $\text{Co}_{75}\text{Si}_{15}\text{B}_{10}$, in the as-quenched state as well as after the low-temperature annealing. The MAE isochrones with characteristic peaks related to different relaxation mechanisms were obtained in a wide temperature range, from which characteristic activation energy spectra of the MRs were calculated.

All samples were produced by the melt spinning tech-

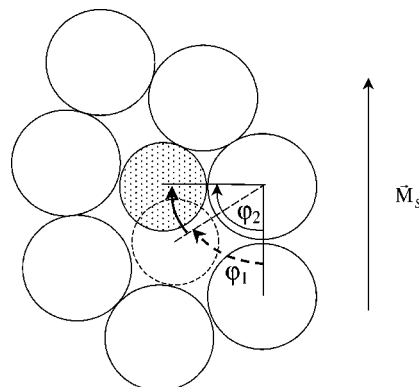


FIG. 1. Reorientation of the atom-pair axis during the structural magnetic relaxation, minimizing the free energy of the system. \vec{M}_s is the local magnetization, φ_1 is the initial angle, φ_2 is the final angle.

nique in the form of 1 mm narrow ribbons. The amorphicity was checked by x-ray diffraction. The time dependences of the initial reluctivity was measured by a PC controlled automatic apparatus based on the *LC* oscillator technique¹³ in the time interval 1–180 s after demagnetization. Temperatures from the region of 100–623 K were stabilized with accuracy ± 0.1 K. The MAE spectrum is represented by a set of temperature dependences of the relative changes of reluctivity $\Delta r(T)/r_1 = [r(t_2) - r(t_1)]/r(t_1)$, $t_1 = 1$ s, $t_2 = 2, 3, 5, 10, 20, 30, 60, 90, 120,$ and 180 s so-called isochrones. The MAE spectra were measured for as-cast samples as well as for annealed ones. The Curie temperature T_C of the amorphous $\text{Co}_{75}\text{B}_{25}$ alloy exceeds its crystallization temperature $T_x = 683$ K, for $\text{Co}_{75}\text{Si}_{15}\text{B}_{10}$ $T_C = 663$ K and $T_x = 750$ K. The samples $\text{Co}_{75}\text{B}_{25}$ were annealed at 653 K and the samples $\text{Co}_{75}\text{Si}_{15}\text{B}_{10}$ at 683 K. Annealings were performed in the argon atmosphere for 1800 s.

The relaxation process in an amorphous alloy is generally characterized by an asymmetric continuous spectrum of the activation energies (AES). A real distribution function of the activation energies $p(Q)$ can be approximated by a set of “*i*” box-type distribution functions with $p(Q_i)$ constant in *i*th interval $(Q_{i,1}, Q_{i,2})$. The fitting function for the measured MAE spectrum $r(t, T)/r_1$ gives such an approximated AES $p(Q)$ for the given amorphous alloy. We have derived such a stepwise AES from an expression for the time dependence of reluctivity¹⁴

$$r(t, T) = r_0(T) + \sum_j \sum_i \Delta r_{ij} \frac{Ei(-t/\tau_{ij,2}) - Ei(-t/\tau_{ij,1})}{\ln(\tau_{ij,2}/\tau_{ij,1})} \quad (3)$$

$$\tau_{ij,2} = \tau_{0j} \exp(Q_{i+1}/kT) \text{ and } \tau_{ij,1} = \tau_{0j} \exp(Q_i/kT), \quad (4)$$

where *j* means a number of the particulate relaxation processes, Ei is an exponential integral $Ei(-x) = -\int_x^\infty [(e^{-u})/u] du$, and τ_{0j} is the relevant preexponential factor. Values $p_j(Q_i)$ were calculated using the least-squares method and the equation $p_j(Q_i) = \Delta r_{ij} / \sum_{i=1}^n \Delta r_{ij}$.

No AES of a simple amorphous Co-based alloy has been presented till now. The MAE spectrum of the investigated amorphous $\text{Co}_{75}\text{B}_{25}$ alloy in the as-cast state can be seen in Fig. 2(a). The MAE spectrum consists from a set of isochrones distinguished one from one another by the time t_2 . Individual isochrones are characterized by their heights (the MAE intensity) and temperatures of their peaks. The 180 s isochrone was chosen as a reference. The MAE spectrum of the CoB amorphous alloy is characterized by a single 38% high peak situated to the temperature $T_p = 383$ K with a half-width $\Delta T = 118$ K (Table I). The shifts of the isochrones peaks to lower temperatures are seen for the increasing t_2 which is typical for the MAE governed by the magnetic relaxation.

The continuous spectra of the activation parameters were supposed in the amorphous alloys.¹⁵ The stepwise AES of the amorphous $\text{Co}_{75}\text{B}_{25}$ alloy—Fig. 2(b)—was obtained by computer fitting the curves of the MAE spectrum with the assistance of formula (3). The number of relaxation types was chosen $j=1$ in Eq. (3) because the only metalloid element “B” is present in the alloy. The activation energy axis

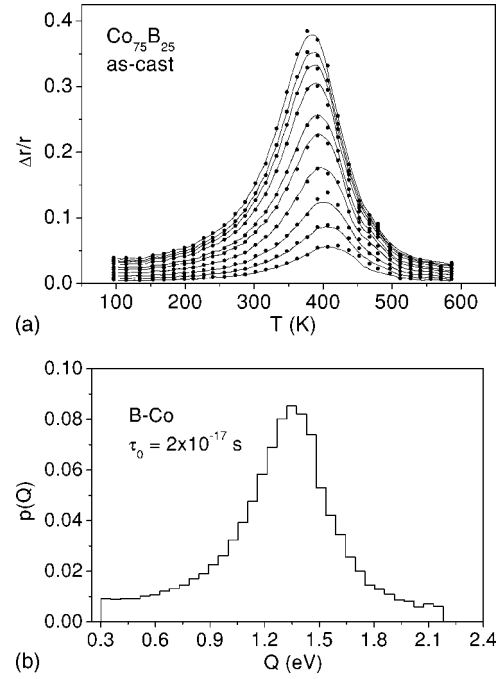


FIG. 2. The amorphous $\text{Co}_{75}\text{B}_{25}$ alloy in the as-cast state (a) the MAE spectrum for $t_1 = 1$ s and $t_2 = 2, 3, 5, 10, 20, 30, 60, 90, 120,$ and 180 s; (.....) are the measured points, (—) is the fit (b) the AES calculated from the MAE spectrum on Fig. 2(a).

was divided into 30 intervals. The obtained AES is characterized by a wide continuous distribution from 0.3–2.18 eV with a relatively narrow peak at the most probable value of the activation energy $Q^* = 1.35$ eV. The best fit gives the preexponential factor in the Arrhenius formula (2b) $\tau_0 = 2 \times 10^{-17}$ s for the amorphous $\text{Co}_{75}\text{B}_{25}$ as-cast alloy. Its small value is attributed to large hopping entropy in Eq. (2c). It indicates that the MR is due to reorientations of the atom-pair axes with respect to the local magnetization.

In the amorphous $\text{Co}_{75}\text{B}_{25}$ alloy, the atom pairs B-Co and Co-Co exist. The existence of B-B pairs is rather improbable because they do not occupy the nearest-neighbor sites.¹⁶ In our case, the narrow MAE spectrum and the consequent AES indicate the only dominant relaxation process. The Co-Co

TABLE I. Parameters of the MAE spectra and the AESs: The asterisk denotes as-cast, the double asterisks denote annealed, MR is the type of the MR, τ_0 is the preexponential factor, Q^* is the most probable activation energy, $\Delta r/r_0$ is the intensity of the MAE, T_p is the temperature of the MAE peak, and ΔT is the half-width of the peak.

Sample	MR	τ_0 (s)	Q^* (eV)	$\Delta r/r_0$ (%)	T_p (K)	ΔT (K)
$\text{Co}_{75}\text{B}_{25}^*$	B	2×10^{-17}	1.35	38	383	118
$\text{Co}_{75}\text{Si}_{15}\text{B}_{10}^*$	B	7×10^{-17}	1.31	10,2	383	120
	Si	6×10^{-18}	1.96	7,2	545	175
$\text{Co}_{75}\text{B}_{25}^{**}$	B	9×10^{-16}	1.55	9.3	478	200
$\text{Co}_{75}\text{Si}_{15}\text{B}_{10}^{**}$	B	2×10^{-15}	1.38	8.3	442	123
	Si	3×10^{-17}	2.01	5,6	576	120

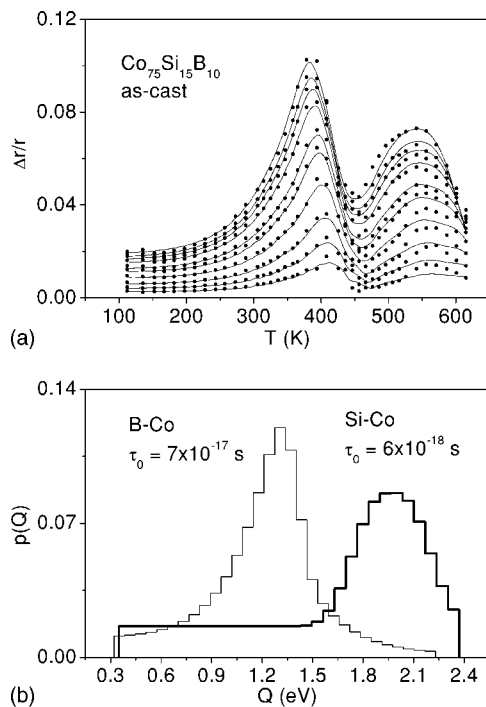


FIG. 3. The amorphous $\text{Co}_{75}\text{Si}_{15}\text{B}_{10}$ alloy in the as-cast state (a) the MAE spectrum, [see Fig. 2(a)]; (b) is the respective AES.

atom-pair reorientation needs much higher activation energy. That means that the MAE in the amorphous $\text{Co}_{75}\text{B}_{25}$ alloy with the peak at 383 K is caused by the magnetic reorientation of the B-Co atom pairs called “the magnetic relaxation of B type.”

The MAE is sensitive on the nearest neighborhood of the migrating atoms. The partial substitution of B by Si dramatically changes the shape of the MAE spectrum [Fig. 3(a)]. The MAE spectrum of the amorphous $\text{Co}_{75}\text{Si}_{15}\text{B}_{10}$ alloy consists of two peaks situated at 383 and 545 K with the intensities 10.2% and 7.2% and the half-widths 120 and 175 K, respectively. Substitution of the B by Si atoms reduces the first MAE peak without affecting its position. It is legitimate to assume that the respective MR is realized by the B-Co atom-pairs reorientations like in the $\text{Co}_{75}\text{B}_{25}$ alloy. We identified the first peak in the $\text{Co}_{75}\text{Si}_{15}\text{B}_{10}$ MAE spectrum as a result of the B-type MR.

Substitution of the B atoms by Si causes formation of the second relaxation peak at 545 K, which is connected with a relaxation process that is not present in the $\text{Co}_{75}\text{B}_{25}$ alloy. This MAE peak cannot be induced by the magnetic transition.¹⁷ Its temperature is well below the Curie temperature ($T_C=663$ K). Its width is much larger than that caused by the phase transition. Even though the Curie temperatures of both alloys are very close, the second MAE peak is created only in the alloy with Si. We conclude that the second MAE peak is originating from the Si-Co atom-pair reorientations, which could be called “the magnetic relaxation of Si type.”

The numerical analysis of the MAE spectrum obtained for the amorphous $\text{Co}_{75}\text{Si}_{15}\text{B}_{10}$ alloy gives two separated AESs [Fig. 3(b)]—one for the B-type MR and the second for the Si-type MR. The fitting of the obtained MAE spectrum by

means of Eq. (3) was performed with the two preexponential factors $\tau_{0j}, j=1$ and 2. The preexponential factor $\tau_{01}=7 \times 10^{-17}$ s was found for the B-Co pairs reorientations, which is in agreement with τ_0 found from the $\text{Co}_{75}\text{B}_{25}$ spectrum analysis ($\tau_0=2 \times 10^{-17}$ s). The agreement in τ_0 indicates similar configurations of the B-Co atom pairs in both sample compositions. This finding is supported by the almost identical AESs in both cases [compare Fig. 2(b) and the left inset in Fig. 3(b)]. The AES for the B-type MR in the CoSiB alloy has the most probable activation energy $Q_1^*=1.31$ eV. The AES for the Si-type MR caused by the Si-Co atom-pair axes reorientations in the amorphous CoSiB alloy [Fig. 3(b)—right inset] was calculated with the preexponential factor $\tau_{02}=6 \times 10^{-18}$ s. The obtained AES is characterized by a wide continuous distribution of the activation energies from 0.32–2.37 eV with a peak at the most probable value $Q_2^*=1.96$ eV. A part of the Si-type MR processes with the activation energies from 0.35–1.42 eV is realized by a constant probability, which is typical for tunnelling-controlled rearrangements in the amorphous structure.

The MAE and AE spectra of the CoB (Fig. 2 and Table I) and FeB¹⁴ amorphous alloys are very similar. Because of the weaker affinity of the B atoms for Co than for Fe,^{19,20} the MAE in the CoB alloy is characterized by a lower activation energy Q^* and its peak is situated at a lower temperature than in the FeB amorphous alloy.

There are remarkable differences between the MAE and AE spectra of the CoSiB (Fig. 3 and Table I) and FeSiB^{14} amorphous alloys. They show two peaks for the CoSiB alloy but only one for the FeSiB alloy. Both alloys contain the B and Si atoms which participate in the MR. The Si atoms shift the MAE of the CoSiB alloy to higher temperatures, similar to the amorphous FeSiB alloy.^{14,18} Since the Si atoms are much larger than B and have a stronger affinity for the Co atoms than for the Fe ones,^{19,20} the shift of the MAE peak towards higher temperatures and the shift of the activation parameters to higher values are much more expressive in the CoSiB alloy than that in the alloy based on Fe. Their relaxation maxima are visibly separated each from another, contrary to the FeSiB alloy.

The influence of the low-temperature annealing on the MAE in the amorphous Co-based alloys was also investigated. The main results are summarized in Table I. The intensity of the MAE spectrum of the amorphous $\text{Co}_{75}\text{B}_{25}$ alloy annealed at 653 K for 1800 s is lowered four times, compared to the as-cast sample. The peak of the spectrum is shifted by 95 K to the temperature 478 K and is made wider to 200 K. The most probable activation energy is increased to 1.55 eV and the preexponential factor to 9×10^{-16} s. The preexponential factor is a structurally sensitive parameter. Its increase means a change of the alloy structure closer to a crystalline one, in which τ_0 is usually on the order 10^{-13} s.⁴

The MAE spectrum of the amorphous $\text{Co}_{75}\text{Si}_{15}\text{B}_{10}$ alloy annealed at 683 K for 1800 s consists again of two peaks located at 442 K for the B-type MR and at 576 K for the Si-type MR. Their maximum intensities are 8.3 and 5.6%, the half-widths are 123 and 120 K, respectively (Table I). The attenuation of the second peak results from the close T_C . Both peaks are shifted to higher temperatures and have reduced intensities, which are typical features of the low-

temperature annealing effect. Compared with the CoB alloy, the relative and absolute changes of the mentioned parameters are much lower. It shows the stabilization effect of the Si substitution on the structure of the Co-based amorphous alloys and the higher resistance of the Si-Co pairs against the low-temperature annealing.

This result is supported by the relatively small shifts of the B-Co and Si-Co AES peaks to higher temperatures and by changes of respective preexponential factors (Table I). The B-Co peak of the AES is shifted only by 0.07 eV to $Q_1^* = 1.38$ eV at $\tau_{01} = 2 \times 10^{-15}$ s. The peak of the Si-Co AES is shifted by 0.05 eV to $Q_2^* = 2.01$ eV at $\tau_{02} = 3 \times 10^{-17}$ s.

The annealing influence on our Co-based amorphous alloys agrees with the free volume conception of the MAE.^{5,21} The annealing causes the free volume release and lowering of the mobile atom-pair's concentration, which results in lowering the MAE peaks, in their shifts to higher temperatures and in an increase of the MR activation energies (Table I). The increase of the preexponential factors after annealing indicates a decrease of the amorphous system entropy and changes in the amorphous microstructure towards the crystallinelike one.

In summary, the paper demonstrates that the MAE spectrum of the amorphous Co₇₅B₂₅ alloy shows a single relax-

ation peak, which corresponds to the B-type MR of the B-Co atom pairs with a broad continuous distribution of the activation energies. The substitution of B by Si brings in the amorphous CoSiB alloy appearance of the second MAE peak at a higher temperature caused by the Si-Co pairs axes reorientations. The Si-type MR is characterized by higher activation energies than the B one. It brings a stronger stabilization influence on the magnetic properties of the amorphous Co-based alloys than the B-type one which is widely exploited in the design of the Co-based amorphous alloys with excellent magnetic properties for technical applications.^{2,3} Our conception of the MR could help to explain the atom-scale origin of the two-hump MAE spectrum of the other multi-component Co-based amorphous alloys, too [e.g., Refs. 9, 14, and 22].

The low-temperature annealing connected with the free volume release brings about the shifts of the MAE peaks to higher temperatures in both alloys and to higher activation energies of both MRs. In both alloys, the increase of the relevant preexponential factors indicates the decrease of the amorphous system entropy and the changes of structural configurations to the more crystallinelike ones.

This work was supported by the scientific VEGA agency, Grants No. 1/8046/01 and 1/1017/04.

*Email address: vojtanik@kosice.upjs.sk

¹R. Hasegawa, *J. Magn. Magn. Mater.* **215–216**, 240 (2000).

²M. Vázquez, *Physica B* **299**, 302 (2001).

³H. Gavrilă and V. Ionita, *J. Optoelectron. Adv. Mater.* **4**, 173 (2002).

⁴H.J. Blythe, H. Kronmüller, A. Seeger, and F. Walz, *Phys. Status Solidi A* **181**, 233 (2002).

⁵H. Kronmüller, *Philos. Mag. B* **48**, 127 (1983).

⁶L. Néel, *J. Phys. Radium* **13**, 485 (1952).

⁷P. Allia and F. Vinai, *Phys. Rev. B* **26**, 6141 (1982).

⁸P. Allia, C. Beatrice, and F. Vinai, *Int. J. Appl. Electromagn. Mater.* **5**, 33 (1994).

⁹G. Buttino, A. Cecchetti, and M. Poppi, *J. Magn. Magn. Mater.* **241**, 183 (2002).

¹⁰P. Vojtanik, M. Boskovicova, E. Kisdi-Koszo, and A. Lovas, *J. Magn. Magn. Mater.* **41**, 385 (1984).

¹¹N. Moser and H. Kronmüller, *Phys. Lett.* **93A**, 101 (1982).

¹²R.-F. Xu, H.-Q. Guo, B.-G. Shen, and L.-Y. Yang, *Phys. Rev. B* **48**, 15 829 (1993).

¹³F. Walz, *Phys. Status Solidi A* **8**, 125 (1971).

¹⁴H. Kronmüller, N. Moser, and F. Rettenmeier, *IEEE Trans. Magn.* **20**, 1388 (1984).

¹⁵P. Vojtanik and I.B. Kekalo, *Phys. Status Solidi A* **60**, K45 (1980).

¹⁶F. Rettenmeier and H. Kronmüller, *Phys. Status Solidi A* **93**, 221 (1986).

¹⁷E. Komova, R. Groessinger, P. Vojtanik, and R. Varga, *Mater. Sci. Eng., A* **226–228**, 693 (1997).

¹⁸Y.-Z. Zhang, *J. Magn. Magn. Mater.* **68**, 145 (1987).

¹⁹M.L. Fdez-Gubieda, I. Orue, F. Plazaola, and J.M. Barandiaran, *Phys. Rev. B* **53**, 620 (1996).

²⁰M.L. Fdez-Gubieda, A. Garcia-Arribas, I. Orue, F. Plazaola, and J.M. Barandiaran, *Europhys. Lett.* **40**, 43 (1997).

²¹P. Vojtanik, L. Potocky, M. Boskovicova, E. Kisdi-Koszo, and A. Lovas, *Acta Phys. Slov.* **31**, 109 (1981).

²²R. Andrejco and P. Vojtanik, *J. Magn. Magn. Mater.* **280**, 108 (2004).